ELSEVIER

Contents lists available at ScienceDirect

Tribology International

journal homepage: www.elsevier.com/locate/triboint





Interactive effect between WS₂ films with different structures and space oils for improvement of tribological performance

Zhen Yan ^{a,b}, Haibin Zhou ^{a,b}, Xiao Zhang ^{a,b}, Jian Liu ^{a,b}, Cong Wang ^{a,b}, Xiaolong Lu ^{a,b}, Junying Hao ^{a,b,*}, Xudong Sui ^{a,b,*}

ARTICLE INFO

Keywords: Solid-liquid lubrication WS₂ film Tribological property Lubricating mechanism

ABSTRACT

WS $_2$ films with different structures and space lubricating oils are combined to construct the WS $_2$ /oils composite lubricating systems. Friction and wear of the WS $_2$ /oils systems are mainly studied in vacuum. Results show that WS $_2$ /P201 systems display much lower friction coefficient ($\mu \approx 0.06$) than WS $_2$ /PFPE systems ($\mu \approx 0.11$), which is found to depend on lubricity of oils. Noteworthily, the dense WS $_2$ film of the WS $_2$ /PFPE systems has the lowest wear rate of about $5.6 \times 10^{-6} \, \mathrm{mm}^3 \cdot (\mathrm{N} \cdot \mathrm{m})^{-1}$ although friction coefficient of the system is high. This is due to good wettability of PFPE on the dense WS $_2$ film, whose contact angle is low to 5° . Eventually, the lubricating mechanism of the WS $_2$ /oil systems are revealed via correlating interaction between oil molecules and WS $_2$ crystals.

1. Introduction

With the rapid developments of high-tech industries, single lubricant hardly ensures the high reliability, accuracy and extended operational life of various mechanism assemblies applied in space under harsh working conditions [1–3]. The solid-liquid lubricating materials can combine with the respective advantages and gradually be attempt to meet the special requirements of mechanical assemblies, which has attracted extensive attention recently on how to combine or match solid/liquid lubricants and further investigate their tribological properties [4–7].

 MoS_2 and WS_2 are the typical lamellar transition metal dichalcogenide with strong covalent bond in the sandwich layer structure and weak van der Waals interaction between the interlayers, leading to the very low shear strength and excellent lubricating property in vacuum [8,9]. The sputtered MoS_2 and WS_2 films have been widely used in the field of aerospace due to the distinct lubrication superiority [10,11]. Although a large number of studies mainly carried out to improve tribological properties of the films via the nanocomposite and multilayer design or optimization [12–14], the films still are easy to wear and exhibit the limited life after long-term sliding test or under severe condition.

It is well known that the surfaces of WS2 and MoS2 crystals possess

basal plane and edge plane. Early several studies reported that some lamellar powders like MoS_2 , WS_2 and graphite have strong affinities with liquid hydrocarbon compounds, such as paraffinic [15,16]. It was found that the liquid compounds with different hydrocarbon chains have different adsorption property on the basal and edge planes of MoS_2 and WS_2 powders. The strong affinity of the surfaces of these crystals is expected to probably affect the lubrication action of these crystals.

Based on those, several studies have been reported by Quan et al. on the tribological performances of WS₂-based films/lubricating oils solidliquid composite systems [17,18]. The results indicate that the tribological properties of the WS2-based films/lubricating oils obtain markable improvement when the films coupled with the space oil with long hydrocarbon chain, such as SiCH (silahydrocarbons) and MACs (multialkylated cyclopentanes), and those composite systems exhibit a low and stable friction coefficient about 0.05-0.08 for these films with different components. But the reverse result is obtained trifluorinated-propyl and chlorinated-phenyl with methyl terminated silicone oil (FCPSO) were used to combine with the WS2-based films, and the difference is found to result from preferential adsorption of oil molecule on the basal and edge planes [17]. Mutyala et al. investigated the tribological properties of Ti-MoS2 films deposited on disk and spherical rolling elements in the boundary-lubricated (PAO ISO 10 oil)

E-mail addresses: jyhao@licp.cas.cn (J. Hao), suixudong@licp.cas.cn (X. Sui).

a State Key Laboratory of Solid Lubrication, Lanzhou Institute of Chemical Physics, Chinese Academy of Science, Lanzhou 730000, China

^b Center of Materials Science and Optoelectronics Engineering, University of Chinese Academy of Sciences, Beijing 100049, China

^{*} Corresponding authors at: State Key Laboratory of Solid Lubrication, Lanzhou Institute of Chemical Physics, Chinese Academy of Science, Lanzhou 730000, China.

conditions [19]. The results indicate that friction coefficient of the steel disk coated Ti-MoS $_2$ films decrease to 0.08 compared to 0.12 of uncoated steel disk and the film results in significant improvement in the rolling contact fatigue life of bearing steels in boundary-lubricated condition, attributing to the formation of protective amorphous hydrocarbon films (a-C:H) containing MoS $_2$ precipitates. Our previous study constructed the dual lubricating systems of WS $_2$ -MoS $_2$ composite film sliding against oil-impregnated porous polyimide pin and found the viscosity of lubricating oil and film component having significant influence on the tribological properties of the systems [20].

It can be seen that the film microstructure and type of lubricating oil have important impact on the tribological properties of the transition metal dichalcogenide-based solid-liquid composite systems. It is noticeable that the WS2- or MoS2-based films reported presently in those literatures all performed a loose and large columnar platelet along whole cross-section of the films in the solid/liquid composite systems [17,20]. In comparison with MoS2, WS2 has a higher oxidation resistance temperature (up to 450 $^{\circ}$ C) and a lower friction coefficient in the atmospheric environment. It can be speculated that the WS2 film should exhibit better environmental suitability and might have potential advantage in space application. Therefore, WS2 has attracted extensive attention recently [13]. However, the studies still are unknown on the interactive effects between WS2 film with different dense structures and space oils for improvement of tribological performances in the solid-liquid composite system.

Accordingly, in this study, two different WS_2 films with loose and whole dense structures were deposited. The WS_2 /space oils composite lubricating systems were constructed via spinning-coating technology. The effects of film microstructure and lubricating oil on the tribological performances of those composite lubricating systems were investigated in vacuum, and lubricating mechanism of the WS_2 films/oils composite systems is also explored.

2. Experimental detail

2.1. Film preparation

The WS $_2$ films with different structures were deposited on both substrates of commercial n-type Si and stainless-steel disc (Ø 25 mm \times 8 mm, Ra \sim 25 nm) by Plasma enhanced chemical vapor deposition system (PECVD, BAK760, Highland). The WS $_2$ targets (345 \times 145 \times 8 mm 3 , 99.99 wt% in purity) were utilized as the cathode of radio frequency power. At a base pressure of 1.0×10^{-3} Pa, the substrates' surfaces were etched in argon plasma for 20 min to eliminate possible contaminants. Afterwards, the loose WS $_2$ film was deposited on the substrate under a sputter power of 400 W, Ar flow of 70 sccm, bias voltage of 15 V, argon pressure of 3×10^{-3} Pa and rotation speed of 1 rpm. Deposition duration is 120 min. The dense WS $_2$ film was deposited under a sputter power of 500 W, Ar flow of 60 sccm, bias voltage of 20 V and argon pressure of 2.8×10^{-3} Pa. The substrate sample was located statically in front of the target. Deposition duration is 70 min. The resulted thicknesses of the two films all are about 0.6 μ m.

2.2. Friction and wear tests in vacuum environment

The polyalphaolefin (PAO) and PFPE (perfluoropolyether, Fomblin Y25) oils as typical liquid lubricants for space application are used. The certain amounts of lubricating oils were spined and uniformly formed a layer of oil film on the surfaces of WS $_2$ films to construct the WS $_2$ film/PAO and WS $_2$ film/PFPE composite lubricating systems, respectively. The physicochemical properties of the selected oils are listed in Table 1.

The friction and wear tests were conducted by a ball-on-disk tribometer (State Key Laboratory of Solid Lubrication) under vacuum environment (below 3.0×10^{-3} Pa, $\sim\!25\%$ RH and 25 ± 5 °C). The counterpart is the 9Cr18 steel ball (Ø 6 mm). The applied normal load is 3 N, the rotation speed is 500 r/min and rotational radius is 5 mm. Each

Table 1Physicochemical properties of PAO and PFPE oils.

Parameters	PAO	PFPE
Molecular structure	n 9 n=1~10	$F_3C - \left[\left(\begin{array}{c} OCFCF_2 \\ I \\ CF_3 \end{array} \right)_m - \left(OCF_2 \right)_n \right] OCF_3$
		m+n = 8-45; $m/n = 20-1,000$
Viscosity at 40 °C/ mm ² ·s ⁻¹	147.0	80
Viscosity at 100 °C/ mm ² ·s ⁻¹	18.4	10
Viscosity index	140	113
Density at 20 °C/g⋅cm ⁻³	0.852	1.90

test was conducted three times under the same condition.

2.3. Structure, component, mechanical and tribological property characterization

The surface morphologies and compositions of the WS2 films, wear tracks and wear scars were charactered by field emission scanning electron microscopy (FESEM, JSM-7610 F, JEOL, Japan), equipped with an energy dispersive spectroscopy (EDS). The crystal structures of the films were measured by X-ray diffraction (GIXRD, EMPYREAN, PANalytical). The nano-hardness and elastic modulus of the film were determined by Nano-Indenter G200 apparatus (MTS, USA) using the Berkovich diamond scratching tip with a taper angle of 90°. The adhesive force of the film-substrate was measured by a scratch test instrument (MFT-4000, Lanzhou Huahui Instrument Technology). Contact angles of the oils on surfaces of the film were measured using a contact angle measurement instrument (DSA 100). Wear volumes and surface roughness of the films were measured by a non-contact 3D profilemeter (MicroMAX-800). The morphologies of the debris collected from wear tracks were examined by transmission electron microscopy (TEM, TECNAI G2 TF20, FEI, USA).

3. Results and discussion

3.1. Film morphology and structure

The loose WS2 film exhibits a porous dendrite-like surface and duplex structure consisting of dense layer near substrate and upper loose columnar layer (Fig. 1a, b). Dentrite surface is typical for the sputtered MoS₂ and WS₂ films [21], mainly attributing to anisotropy of WS₂ crystal and its equiaxed crystal transition [22]. Fig. 1c, d show surface and cross-section FESEM micrographs of the whole dense WS2 films. It can be seen that the dendrite-like platelets of the film become small in size and embed into the dense film. The film presents a whole dense structure. It indicates that adjusting the argon pressures and dwell time of sample on the front of the target is an effective approach to tailor the microstructure of WS2 film. It is attributed that the plasma's bombard effect for the growing film is enhanced due to the long mean free path as the argon pressure decreased [23]. The surface roughnesses are approximate and about 30 nm for the loose and whole dense WS₂ films. For the WS₂ film/oil systems, an oil film is evenly spread out the surface of WS2 film.

Fig. 2 gives the typical GIXRD patterns of the loose and whole dense WS_2 films. The films can be identified as 2 H-WS₂ phase (JCPDS card no. 08–0237). The loose WS_2 film mainly shows two diffraction peaks that correspond to the textures of edge planes (100) and (110) of WS_2 , respectively. In comparison to the loose WS_2 film, the whole dense WS_2 film shows a low and broad peak of (100) texture, whose intensity

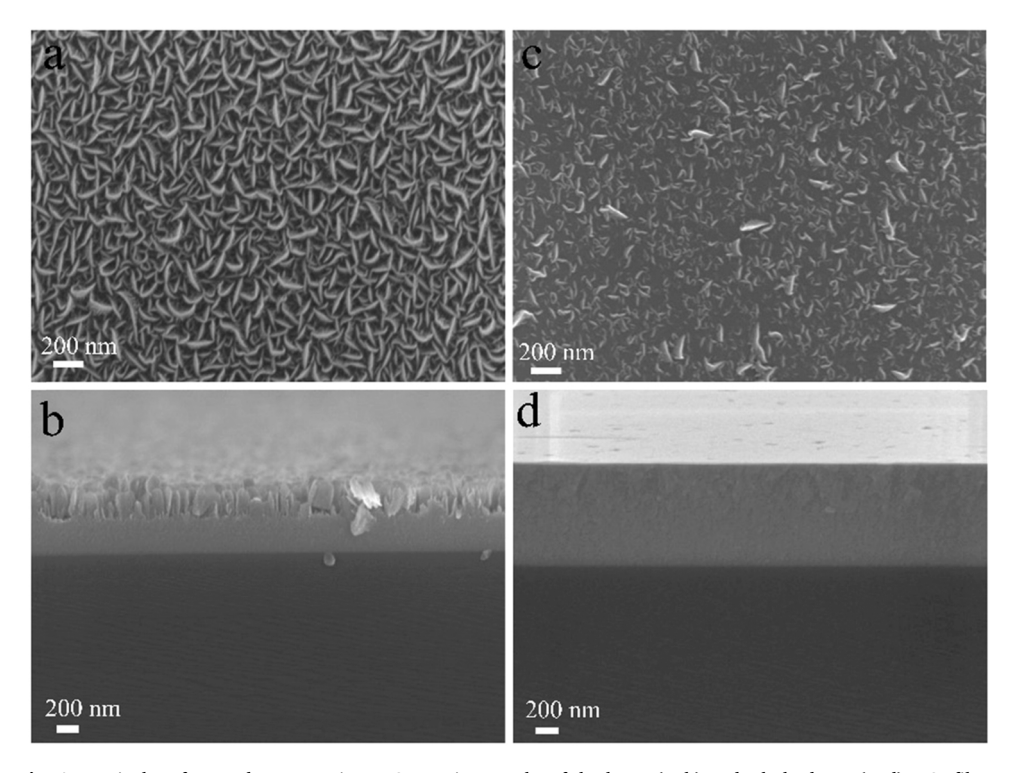


Fig. 1. Typical surface and cross-section FESEM micrographs of the loose (a, b) and whole dense (c, d) WS2 films.

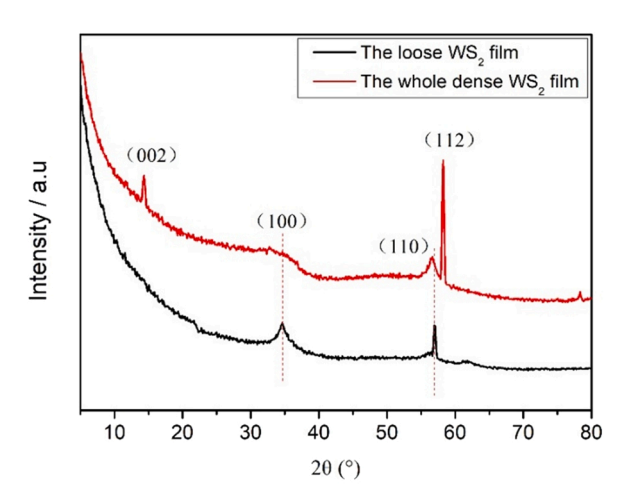


Fig. 2. GIXRD patterns of the loose and whole dense WS_2 films.

obviously decreases and the full width at half maximum (FWHM) increases, suggesting crystallite reorientation [24]. It is attributed that the WS $_2$ crystal grain size with (100) orientation become smaller and the turbostrating stacking of the S-W-S sandwich interlayer presents in the film [25]. The weak (002) and strong (112) peaks appear including weak (110) peak, indicating that parts of WS $_2$ crystals grew in the basal plane orientation and edge plane of (112) in film is preferential growth [22]. It makes film become densifying.

3.2. Mechanical properties

The hardness, elastic modulus and elastic index of the WS_2 films are depicted in Fig. 3. It can be seen that the hardness and elastic modulus of the loose WS_2 film are 0.15 GPa and 13.6 GPa, respectively, which is common for sputtered WS_2 film reported presently [26]. For the whole dense WS_2 film, the hardness and elastic modulus are 7.5 GPa and 109 GPa, respectively. The values are far higher than those of sputtered

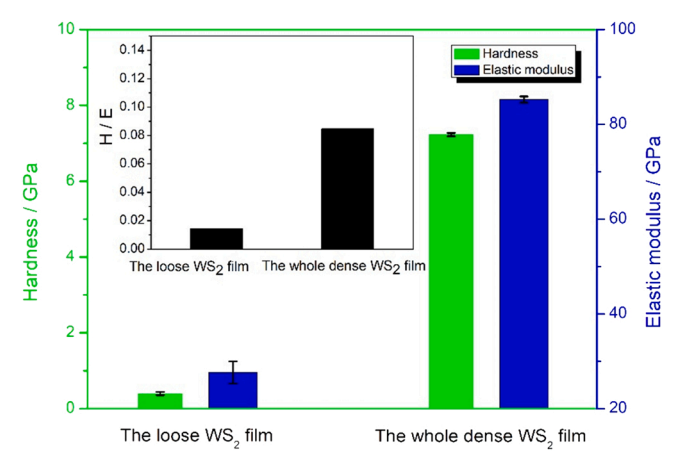


Fig. 3. The hardness and elastic modulus of the WS₂ films.

pure WS_2 or MoS_2 films with good crystalline in the reported studies [27–29]. The elastic index (H/E) is used to evaluate the elastic behavioral limit of surface contact and resistance plastic deformation of material [30,31]. It is concluded that the whole dense film exhibits much higher hardness, elastic modulus and higher H/E ratio compared to the loose WS_2 film.

The scratch tests were measured to evaluate adhesion of film-substrate of the WS $_2$ films under a linearly increasing load from 0 N to 20 N and loading speed of 15 N/min. The friction force curves and optical images of the scratch tracks for the WS $_2$ films are shows Fig. 4. It can be seen that the friction force curves dose not exhibit obvious fluctuation with increase of loading force due to good lubricity of the film, which cannot use to determine the critical load value. From scratch track images, the white areas inside the worn track are the film spallation region at the critical load. The loose film shows obvious plastic deformation, and the thin cracks and film spallation occurred when the adhesion force reached to about 12 N (Fig. 4a). Differently, for the whole dense film, slight cracks and film spallation are observed at the adhesion force 18 N

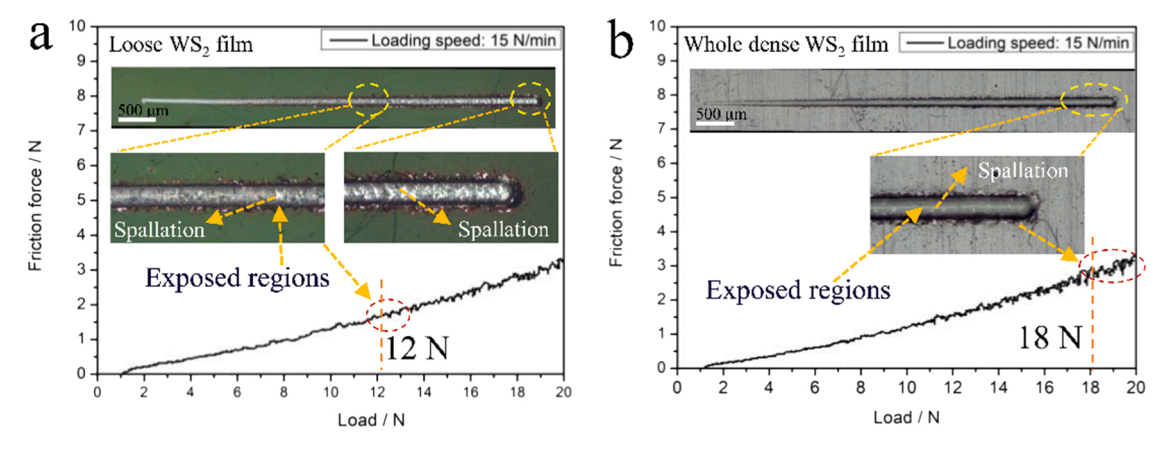


Fig. 4. The friction force curves and optical images of the scratch tracks for the loose (a) and whole dense (b) WS₂ films.

near the end of the scratch track (Fig. 4b). It indicates the whole dense WS_2 film have much better adhesion and resistance plastic deformation, meaning more excellent mechanical property.

3.3. Tribological property

In order to firstly evaluate the natural friction coefficient of the PFPE and P201 oils, the enough oil amount was used to fully overspread on the surface of steel substrate. It can be seen that the friction coefficient of PFPE oil is much higher than that of P201 oil in vacuum shown in Fig. 5a. The PFPE oil exhibits a transient high friction at the initial running-in stage and then friction coefficient stabilizes at 0.16 when the continuous oil film was formed on the contact area of the steel/steel tribo-pair, in accordance with the related study [32]. However, P201 oil shows a low and stable friction coefficient of 0.08. It can be concluded that P201 oil have more excellent lubricating property and lower shear force among oil molecules in comparison with PFPE oil. Fig. 5b gives the friction coefficient curves and wear life of the loose and whole dense WS₂ films under the dry friction condition. It can be seen that the two WS₂ films exhibit similar friction coefficient of about 0.02. The average wear life is about 6.2×10^4 r and 8.8×10^4 r for the loose and dense WS₂ films, respectively, indicating that the dense WS₂ film exhibits greater life than the loose film. It verified that the whole dense film possesses more excellent lubricating property.

Generally, proper combination of solid and liquid lubricants can produce a significant improvement for the tribological performance in comparison with the single lubricant. Fig. 6 shows the typical friction curves of the loose WS $_2$ film/oils and whole dense WS $_2$ films/oils systems in vacuum. It can be seen that for the loose WS $_2$ film, the friction coefficients of the WS $_2$ /P201 and WS $_2$ /PFPE systems are about 0.10 and

0.05, respectively. For that dense film, the friction coefficients of the WS $_2/P201$ and WS $_2/PFPE$ systems slightly increase compared to the loose WS $_2$ film in the solid/oil systems. It indicates that the WS $_2/P201$ systems have more excellent lubricating property than the WS $_2/PFPE$ systems, which mainly depends on natural lubricity of the oils. The results also indicate that densification of the WS $_2$ film has no obvious influence on the friction in the solid-liquid interface and the friction of the two films in the WS $_2/oil$ systems appear virtually the same.

Fig. 7 shows the average friction coefficients and wear rates of the WS_2 films in the WS_2 /oils composite systems and the dry friction condition. It can be seen that lubricating oils and film structure have different influence on the average friction coefficients and wear rates of the two films. WS_2 /PFPE systems show the highest average friction coefficients. In comparison with the loose film, the average friction coefficient of whole dense WS_2 film slightly decreases in the dry friction condition. Inversely, it all slightly increase in the solid/oils systems for the dense WS_2 film (Fig. 7a).

In terms of the average wear rates (Fig. 7b), it decreases 60% for dense WS_2 film compared to the loose film in the dry friction condition, indicating that wear resistance of the dense WS_2 film is evidently enhanced. It is attributed to the dense microstructure, better adhesion and resistance plastic deformation of the whole dense WS_2 film. The loose WS_2 film shows lower wear rate compared to the whole dense WS_2 film in the $WS_2/P201$ system. Differently, the whole dense WS_2 film exhibits the lower wear rate in the $WS_2/PFPE$ system. Therefore, it indicates that the loose WS_2 film has better wear resistance in the $WS_2/P201$ system and the whole dense film has better wear resistance in the $WS_2/PFPE$ system. Similar results also are reported that the loose WS_2 film with large columnar platelets combined with PAO oil obviously decrease the wear of the film [17,33]. It indicates that the WS_2 film with

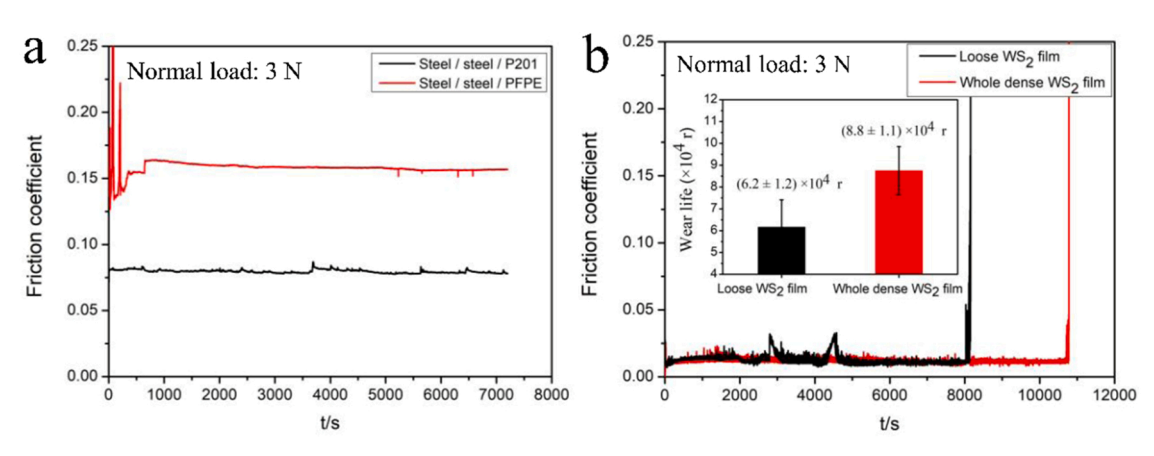


Fig. 5. Friction curves of single lubricating oil (a) and the loose and whole dense WS2 films (b) as function of sliding time in vacuum (inset the wear life of film).

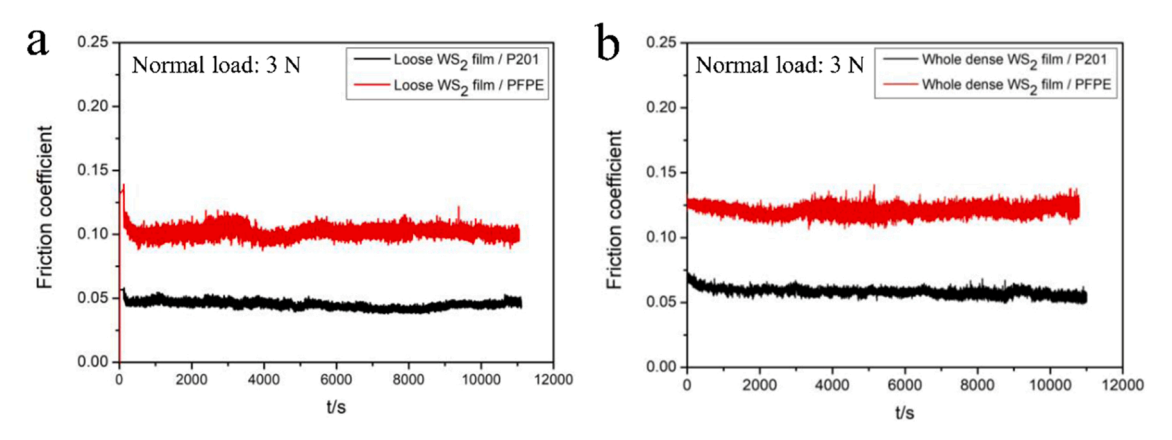


Fig. 6. Friction curves of the loose WS2 films/oils (a) and whole dense WS2 films/oils (b) systems in vacuum.

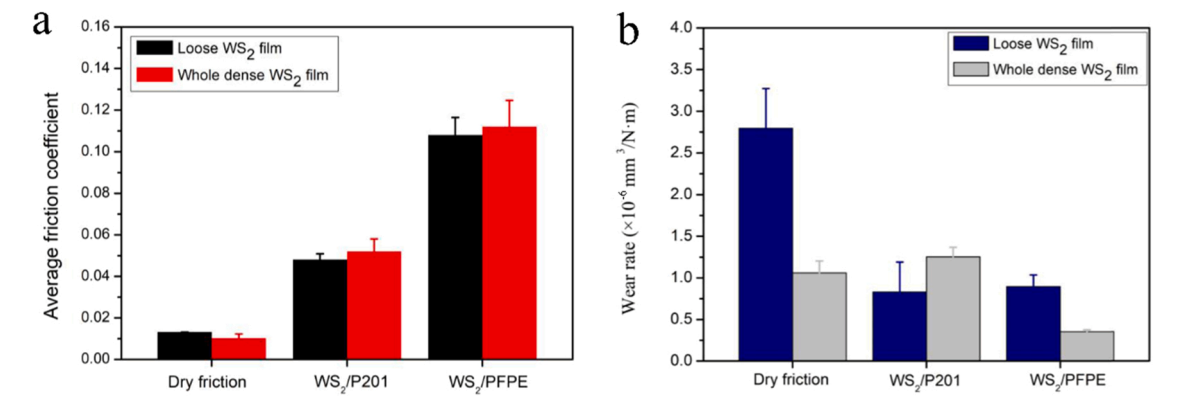


Fig. 7. The average friction coefficients (a) and wear rates (b) of the WS2 films in the WS2/oils composite systems and the dry friction condition.

loose structure is more favorable to decrease the wear of film in the solid/oil composite system, but when the microstructure of WS_2 film becomes densifying, the film lubricated with PFPE oil is more favorable to decrease the wear of film.

3.4. Lubricating mechanism

In order to study the interaction between WS_2 films and oils for

improvement of tribological performances in the solid-liquid systems, the wear tracks and corresponding scars for the loose and whole dense WS_2 films are firstly investigated, as shown in Fig. 8. It can be seen that the wear track of whole dense film becomes narrower and the scratches and groove becomes less (Fig. 8b1, b2) compared to that of the loose film under dry friction condition (Fig. 8a1, a2), confirming more excellent wear resistance for the whole dense film. Besides, there are amounts of wear debris inside and at the edge of the wear track for the two films,

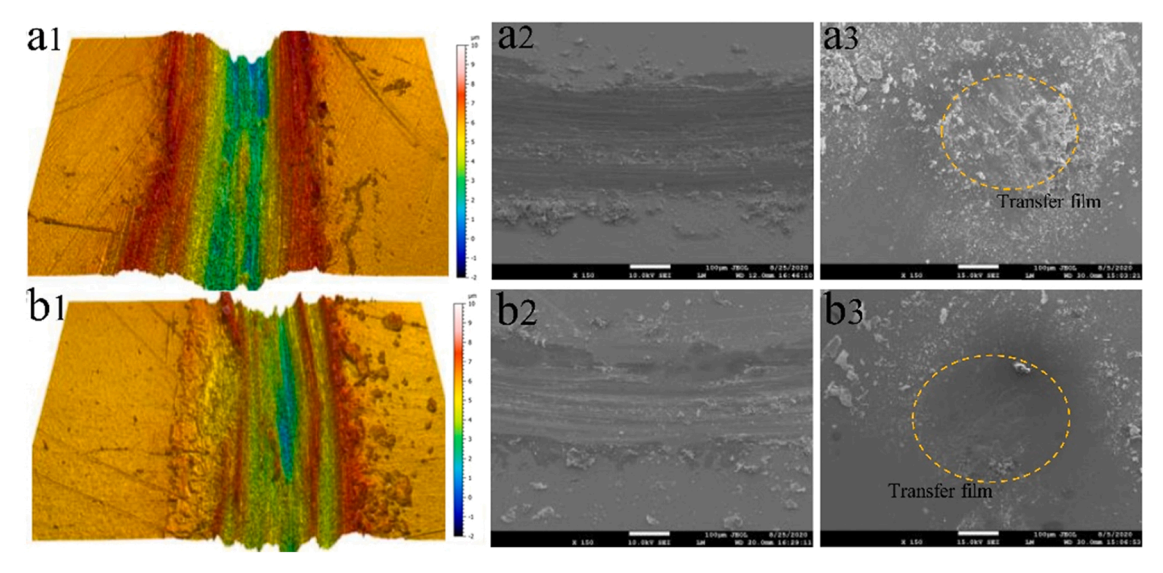


Fig. 8. FESEM images of the wear tracks and corresponding scars for the loose (a1-a3) and whole dense (b1-b3) WS2 films under dry friction condition.

and more transfer film is clearly observed on the wear scar for the loose film (Fig. 8a3). It indicates that film structure has significant influence on the wear behavior of the lamellar solid film.

For the WS_2 films/oils systems, the lubricating oils remaining on wear track were cleaned using solvent and then used to analyze wear tracks. Fig. 9 shows FESEM images of the wear tracks for the loose and whole dense WS_2 films/oils systems. A common character is noticed for these WS_2 /oil systems, wear tracks become relatively smooth and scratches obviously disappear. It indicates that strong interaction occurred between WS_2 crystal planes and oil molecules.

Noteworthy, the film structure and oil medium have obvious impact on the wear of the film. For the loose film, some scour pits inside the wear track can be observed and parts of flake-like debris or fragments adhere to the wear track owing to film detachment for the film/P201 system (Fig. 9a). However, for the dense film/oils systems (Fig. 9c, d), some pits and scratches are clearly observed on the wear track. The maximum depth of worn track is larger in the WS₂/P201 system and becomes smaller in the WS₂/PFPE system compared to the loose WS₂ film. It indicates that the interaction between oil molecules and WS₂ crystals is different and affects the wear of the two films. The results also confirm that the P201 and PFPE oils must preferentially adsorb on the different planes of WS₂ crystals, where the crystal planes adsorbed by P201 oil are easy to slip and the crystal planes adsorbed by PFPE oil are slipped difficultly.

The wear scars of the counterpart balls after friction tests were also examined. Fig. 10 shows the optical images of the wear scars on steel ball sliding against the loose and dense WS $_2$ films/oils composite systems. For the loose film, a bit of shallow furrows and black debris can be observed on surface of wear scar due to plowing function of debris for the film/P201 system (Fig. 10a), while the number of furrows becomes more for the film/PFPE system (Fig. 10b), in good accordance with morphologies of corresponding wear tracks. In comparison with the loose film, the sizes of wear scars are larger and the number of furrows significantly increases accompanying some debris squeezed into the furrows for the dense film (Fig. 10c, d). It is attributed that the dense film seemingly tends to form hard particles plowing the contact area during the friction test.

In the solid-liquid composite system, it is well-known that wettability of liquid lubricant with solid lubricant has important influence on the friction and wear of the system as well as generation of synergistic lubricating effect [2,7,34]. The wettability of PFPE and P201 oils with the WS2 films was assessed by measuring the contact angles at room temperature (25 °C) by injecting 4 μl oil. Fig. 11 gives the values and images of contact angle of the two oils on surfaces of the loose and dense WS2 films. It can be seen that the contact angles of PFPE and P201 oils are similar and about 9° on the surface of the loose film, indicating the two oils have good wettability with the loose film. Differently, the contact angle is low to 5° for PFPE oil while is high to 14° for P201 oil on the surface of the dense film. It illustrates that PFPE oil molecules with C-F chain are easier to combine and absorb with the dense film, thereby resulting in low wear rate for the dense film due to formation of an oil layer on the contact zone.

For the sake of further elucidating the lubricating mechanism of the WS2 films/ oil systems, the debris inside the wear track were examined by TEM. Fig. 12 shows the TEM images of the debris for single whole dense WS2 film as well as the film/oils systems after friction tests. It can be seen that the debris of the single dense film presents the large size and black thick platelets (Figs. 12a, a1), while the platelets of debris evidently become thin in the solid-oil systems. For the WS₂/P201 system, the surface of the platelet is uneven and shows many cavities, and the local high-resolution image of the platelet further presents the multiple different crystal orientations in the vicinity of cavities (Figs. 12b, b1). It implies that the P201 oil molecules have strong interaction with planes of WS2 crystals during the slippages and cleavages of WS₂ crystals under shear force. Noteworthily, it is found that the platelets of the debris exhibit a variety of shapes and become fragmentation for the dense WS2 film/PFPE system (Figs. 12c, c1). Meanwhile, a few lattice fringes can be seen on the local high-resolution image of the platelet of the debris, suggesting that P201 oil molecules might appear different absorption strength on the different texture planes of WS2 crystals in the film.

It is well known that the surfaces of WS₂ or MoS₂ crystals consist of basal and edge plane areas. The basal plane of S atoms layer in a hexagonal arrangement has a high aspect ratio and a relatively low surface

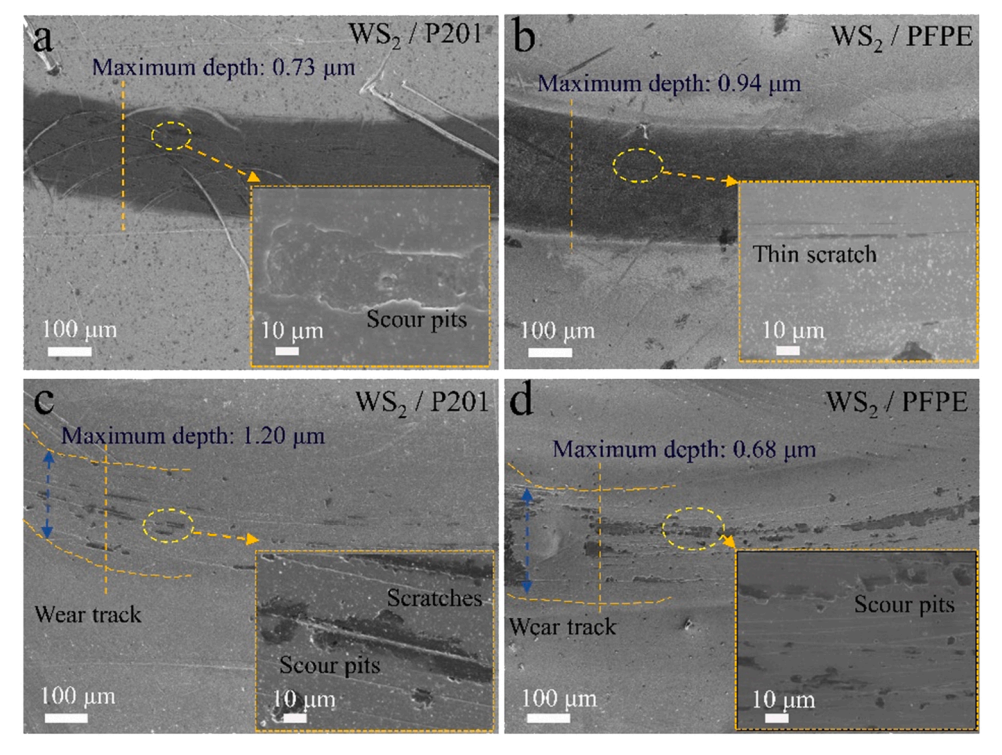


Fig. 9. FESEM images of the wear tracks for the loose (a, b) and whole dense (c, d) WS2 films/oils systems.

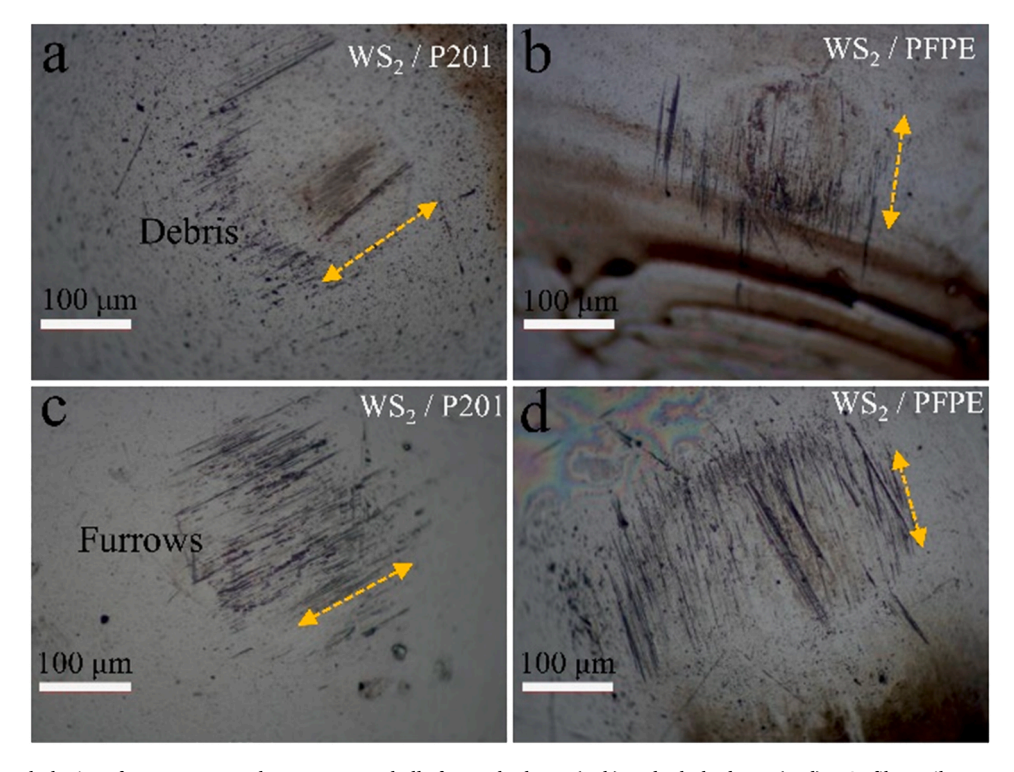


Fig. 10. The morphologies of wear scars on the counterpart balls for W the loose (a, b) and whole dense (c, d) WS2 films/oils systems after the tests.

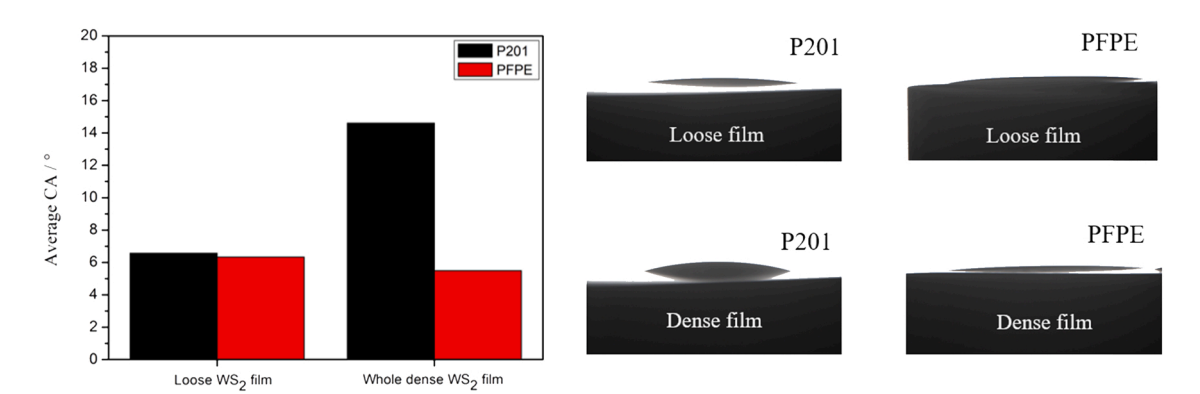


Fig. 11. The values and images of contact angle of the two oils on the surfaces of the loose and dense WS_2 films.

energy as well as non-polarity [35]. It has been reported that lamellar powders like MoS_2 , WS_2 and graphite have strong affinities with liquid paraffins or mineral oils, and normal hydrocarbon could convert powders surface from polar plane to basal plane to some extent via effecting the cleavage of the lamellar crystals during the grinding process [36,37]. Quan et al. revealed whether the lubricating oil first preferentially adsorbed on basal or edge planes, which mainly depend on the carbon hydrocarbon chain structure and polarity of the oil molecules [18].

In fact, for the solid-liquid system, the contact zone of the tribopair is separated by the lubricating oil, mixture layers composed of oil and WS₂ platelets and WS₂ film during the friction tests. The schematic illustration of the lubricating mechanism is shown in Fig. 13. The mixture layer plays a vital role in generating different lubricating effect. Therefore, for the dense WS₂ film/P201 system, compared to the bulky debris under dry friction, the thin plate-like debris confirm that P201 oil molecule strongly absorbed the WS₂ crystal plane. Moreover, the uneven surface exposed multiple different crystal plane of the debris reveals that adsorption force of the P201 oil molecule has different intensities on different crystal planes and thus results in the cleavages of the lamellar crystals at different local position. However, for the whole dense WS₂

film/PFPE system, the debris become strip-like particle and thin fragmentation. PFPE molecule is composed of C-C and C-F chain and is polar, which preferentially adsorbed on the edge planes of WS $_2$ crystals [33]. Cleavages of WS $_2$ crystals are easy to generate along the edge planes absorbed by PFPE molecule. But edge planes of WS $_2$ crystals is difficult to slip and become smaller particles under the shear force. Those smaller particles are not flat during sliding and is easy to further become the fragmentation of WS $_2$ particles. Interestingly, it is favorable to inversely improve friction and wear of the whole dense WS $_2$ film/PFPE system due to formation of continue mixture layer on the surface of the dense WS $_2$ film.

4. Conclusions

The WS_2 films with loose and whole dense structures were prepared and the WS_2 /oils composite lubricating systems were successfully established. Compared to the loose WS_2 film, the whole dense WS_2 film exhibits more excellent mechanical and tribological properties. Results indicates that WS_2 /P201 system shows much lower friction coefficient than that of WS_2 /PFPE system, depending on intrinsic lubricating

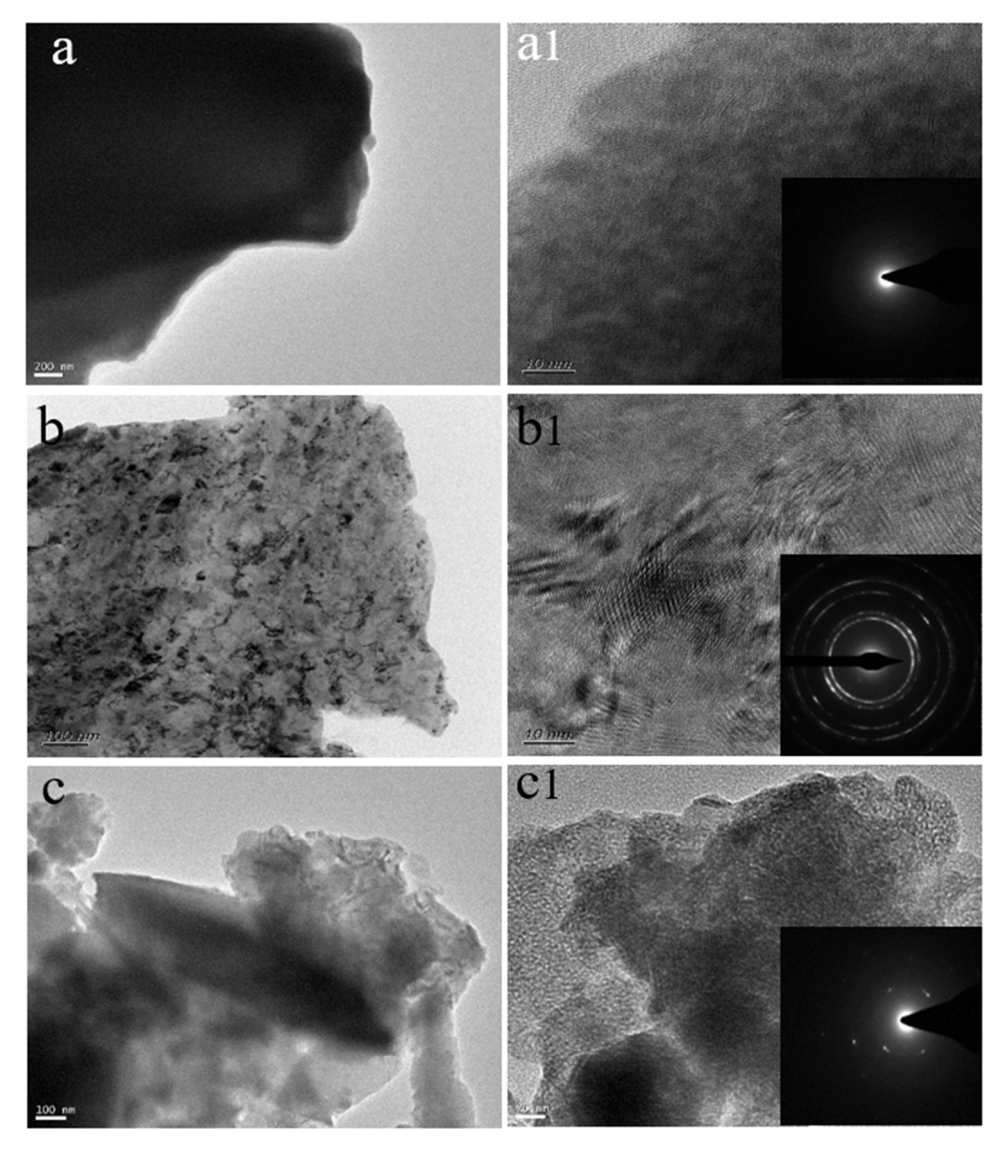


Fig. 12. TEM images of the debris for single whole dense WS_2 film (a, a1) as well as the film/P201(b, b1) and/PFPE (c, c1) oils systems.

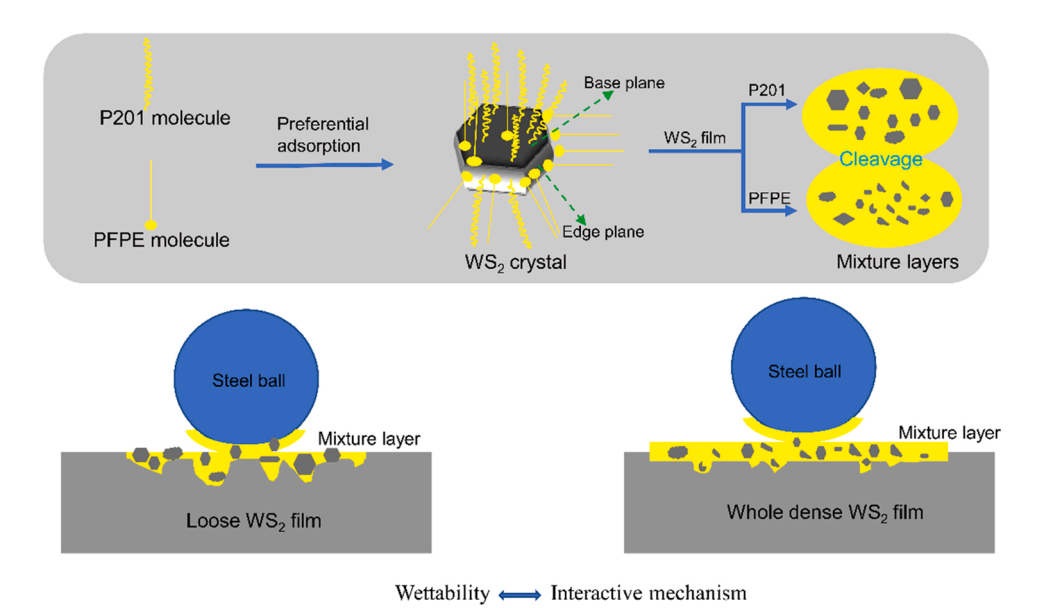


Fig. 13. The schematic illustration of the lubricating mechanism.

properties of neat oils. Differently, the property of oil and film structure generate evident impact on the wear of film in the WS_2 /oil systems. The whole dense WS_2 film/PFPE system inversely displays lowest wear rate although PFPE oil is poor in lubricity compared to P201 oil, which was found to be related to wettability of oils. It is concluded that the whole dense WS_2 film/P201 system has more excellent lubricity and wear resistance, which is the best combination for mechanism assemblies applied in space under harsh working conditions. Meanwhile, it reveals that the interaction among oil, WS_2 platelets and WS_2 film is responsible for lubricity of the WS_2 /oil system. It would provide additional insight on the lubrication design of solid-liquid system in space.

CRediT authorship contribution statement

Zhen Yan: Conceptualization, Investigation, Data curation, Writing – original draft. Haibin Zhou: Methodology, Data curation. Xiao Zhang: Conceptualization, Methodology. Jian Liu: Conceptualization. Cong Wang: Conceptualization, Formal analysis. Xiaolong Lu: Data curation. Junying Hao: Project administration, Supervision, Data curation, Funding acquisition. Xudong Sui: Methodology, Writing – review & editing, Supervision.

Declaration of Competing Interest

The authors declare that they have no known competing financial interests or personal relationships that could have appeared to influence the work reported in this paper.

Acknowledgements

This work was supported by the National Natural Science Foundation of China (51835012, 51975554), National Key R&D Plan of China (No. 2018YFB0703803), CAS "Light of West China" Program and the program of "Science & Technology International Cooperation Demonstrative Base of Metal Surface Engineering along the Silk Road (2017D01003)".

References

- Bedingfield KL, Leach RD. Spacecraft system failures and anomalies attributed to the natural space environment. NASA Ref Publ 1996;1390.
- [2] Fan XQ, Xue QJ, Wang LP. Carbon-based solid-liquid lubricating coatings for space applications-a review. Friction 2015;3(3):191–207.
- [3] Li HM, Yi PY, Zhang D, Peng LF, Zhang ZF, Pu JB. Integration of MoST and GraphitiC coatings for the enhancement of tribological and corrosive properties. Appl Surf Sci 2020;506:1–9.
- [4] Lv M, Yang LJ, Wang QH, Wang TM, Liang YM. Tribological performance and lubrication mechanism of solid-liquid lubricating materials in high-vacuum and irradiation environments. Tribol Lett 2015;59(1):1–10.
- [5] Yu CY, Ju PF, Wan HQ, Chen L, Li HX, Zhou HD, et al. Designing a PAI/PTFE coating with enhanced high-temperature tribological properties by S8-POSS: solidliquid dual lubrication. Prog Org Coat 2020;145:1–11.
- [6] Cyriac F, Yi TX, Poornachary SK, Chow PS. Behavior and interaction of boundary lubricating additives on steel and DLC-coated steel surfaces. Tribol Int 2021;164: 107199.
- [7] Yan MM, Wang XY, Zhang SW, Zhang ST, Sui XD, Li WS, et al. Friction and wear properties of GLC and DLC coatings under ionic liquid lubrication. Tribol Int 2020; 143:1–11
- [8] Hotovy I, Spiess L, Mikolasek M, Kostic I, Sojkova M, Romanus H, et al. Layered WS_2 thin films prepared by sulfurization of sputtered W films. Appl Surf Sci 2021;
- [9] Nicholson E, Serles P, Wang GR, Filleter T, Davis JW, Singh CV. Low energy proton irradiation tolerance of molybdenum disulfide lubricants. Appl Surf Sci 2021;567:
- [10] Marquart M, Wahl M, Emrich S, Zhang G, Sauer B, Kopnarski M, et al. Enhancing the lifetime of MoS₂-lubricated ball bearings. Wear 2013;303(1–2):169–77.

- [11] Todd MJ. Solid lubrication of ball bearings for spacecraft mechanisms. Tribol Int 1982:331–7.
- [12] Lu XL, Yan MM, Yan Z, Chen WY, Sui XD, Hao JY, et al. Exploring the atmospheric tribological properties of MoS₂-(Cr, Nb, Ti, Al, V) composite coatings by high throughput preparation method. Tribol Int 2021;156:106844.
- [13] Xu SS, Liu YZ, Gao MY, Kang KH, Shin DG, Kim DE. Superior lubrication of dense/porous-coupled nanoscale C/WS₂ multilayer coating on ductile substrate. Appl Surf Sci 2019;476:724–32.
- [14] Zhang X, Zhang K, Kang X, Zhang L. Friction maps and wear maps of Ag/MoS₂/ WS₂ nanocomposite with different sliding speed and normal force. Tribol Int 2021; 164:107228.
- [15] Groszek AJ. Preferential adsorption of long-chains mormal paraffins on MoS₂, WS₂ and graphite from n-heptane. Nature 1964;204. 680-680.
- [16] Groszek AJ. Selective adsorption at graphite/hydrocarbon interfaces. Proc R Soc A Math Phys Eng Sci 1970;314.
- [17] Quan X, Gao XM, Weng LJ, Hu M, Jiang D, Wang DS, et al. Tribological behavior of WS₂-based solid/liquid lubricating systems dominated by the surface properties of WS₂ crystallographic planes. RSC Adv 2015;5:64892–901.
- [18] Quan X, Hu M, Gao XM, Fu YL, Weng LJ, Wang DS, et al. Friction and wear performance of dual lubrication systems combining WS₂-MoS₂ composite film and low volatility oils under vacuum condition. Tribol Int 2016;99:57–66.
- [19] Mutyala KC, Singh H, Fouts JA, Evans RD, Doll GL. Influence of MoS₂ on the rolling contact performance of bearing steels in boundary lubrication: a different approach. Tribol Lett 2016;61(20):1–11.
- [20] Yan Z, Jiang D, Fu YL, Qiao D, Gao XM, Feng DP, et al. Vacuum tribological performance of WS₂-MoS₂ composite film against oil-impregnated porous polyimide: influence of oil viscosity. Tribol Lett 2019;67(2):1–10.
- [21] Deepthi B, Barshilia HC, Rajam KS, Konchady MS, Pai DM, Sankar J, et al. Structure, morphology and chemical composition of sputter deposited nanostructured Cr-WS₂ solid lubricant coatings. Surf Coat Technol 2010;205(2): 565–74.
- [22] Spalvins T. Frictional and morphological properties of Au-MoS₂ films sputtered from a compact target. Thin Solid Films 1984;118(3):375–84.
- [23] Chen LM, Tu JP, Zhang SC, Peng SM, Gu B. Effect of deposition pressure on microstructure and tribological behavior of MoS_x/MoS_x-Mo nanoscale multi-layer films. Tribol Lett 2007;25(2):87–91.
- [24] Zabinski JS, Donley MS, Walck SD, Schneider TR, Mcdevitt NT. The effects of dopants on the chemistry and tribology of sputter-deposited MoS₂ films. Tribol Trans 1995;38:894–904.
- [25] Rigato V, Maggioni G, Boscarino D, Sangaletti L, Depero L, Fox VC, et al. A study of the structural and mechanical properties of Ti/MoS₂ coatings deposited by closed field unbalanced magnetron sputter ion plating. Surf Coat Technol 1999;116–119: 176–83.
- [26] Deepthi B, Barshilia HC, Rajam KS, Konchady MS, Pai DM, Sankar J. Structural, mechanical and tribological investigations of sputter deposited CrN-WS₂ nanocomposite solid lubricant coatings. Tribol Int 2011;44(12):1844–51.
- [27] Qin XP, Ke PL, Wang AY, Kim KH. Microstructure, mechanical and tribological behaviors of MoS₂-Ti composite coatings deposited by a hybrid HIPIMS method. Surf Coat Technol 2013;228:275–81.
- [28] Li H, Xie ML, Zhang GA, Fan XQ, Li X, Zhu MH, et al. Structure and tribological behavior of Pb-Ti/MoS₂ nanoscaled multilayer films deposited by magnetron sputtering method. Appl Surf Sci 2018;435:48–54.
- [29] Fu YL, Jiang D, Wang DS, Gao XM, Hu M, Yang W. Tribological performance of MoS₂-WS₂ composite film under the atomic oxygen irradiation conditions. Materials 2020;13(6):1–14.
- [30] He DQ, Shang LL, Lu ZB, Zhang GA, Wang LP, Xue QJ. Tailoring the mechanical and tribological properties of B₄C/a-C coatings by controlling the boron carbide content. Surf Coat Technol 2017;329:11–8.
- [31] Leyland A, Matthews A. On the significance of the H/E ratio in wear control: a nanocomposite coating approach to optimised tribological behaviour. Wear 2000; 246:1-11
- [32] Zeng QF. Superlow friction and diffusion behaviors of a steel-related system in the presence of nano lubricant additive in PFPE oil. J Adhes Sci Technol 2019;33(9): 1001–18.
- [33] Yan Z, Jiang D, Gao XM, Zhang C, Hu M, Feng DP, et al. Tribological behavior of WS₂/oil-impregnated porous polyimide solid/liquid composite system. Ind Lubr Tribol 2019;71(3):459–66.
- [34] Xue YW, Shi XL, Huang QP, Zhang KP, Wu CH. Effects of groove-textured surfaces with Sn-Ag-Cu and MXene-Ti₃C₂ on tribological performance of CSS-42L bearing steel in solid-liquid composite lubrication system. Tribol Int 2021;161:107099.
- [35] Andrews GI, Groszek AJ, Hairs N. Measurement of surface areas of basal plane and polar sites in graphite and MoS₂ powders. ALSE Trans 1972;15:184–91.
- [36] Giltrow JP, Groszek AJ. The effect of particle shape on the abrasiveness of lamellar solids. Wear 1969;13:317–29.
- [37] Groszek AJ. Preferential adsorption of compounds with long methylene chains on cast iron, graphite, boron nitride, and molybdenum disulfide. Tribol Trans 1966;9: 67–76